HHS Public Access

Author manuscript

Toxicology. Author manuscript; available in PMC 2021 February 15.

Published in final edited form as:

Toxicology. 2020 February 15; 431: 152379. doi:10.1016/j.tox.2020.152379.

Multifunctional compounds Lithium Chloride and Methylene Blue attenuate the negative effects of diisopropylfluorophosphate on axonal transport in rat cortical neurons

Sean X Naughton, **Wayne D. Beck**, **Zhe Wei**, **Guangyu Wu**, **Alvin V. Terry Jr.**

Department of Pharmacology and Toxicology, Medical College of Georgia, Augusta University, Augusta, Georgia, 30912

Abstract

Organophosphates (OPs) are valuable as pesticides in agriculture and for controlling deadly vector-borne illnesses; however, they are highly toxic and associated with many deleterious health effects in humans including long-term neurological impairments. Antidotal treatment regimens are available to combat the symptoms of acute OP toxicity, which result from the irreversible inhibition of acetylcholinesterase (AChE). However, there are no established treatments for the long-term neurological consequences of OP exposure. In addition to AChE, OPs can negatively affect multiple protein targets as well as biological processes such as axonal transport. Given the fundamental nature of axonal transport to neuronal health, we rationalized that this process might serve as a general focus area for novel therapeutic strategies against OP toxicity. In the studies described here, we employed a multi-target, phenotypic screening, and drug repurposing strategy for the evaluations of potential novel OP-treatments using a primary neuronal culture model and time-lapse live imaging microscopy. Two multi-target compounds, lithium chloride (LiCl) and methylene blue (MB), which are FDA-approved for other indications, were evaluated for their ability to prevent the negative effects of the OP, diisopropylfluorophosphate (DFP) on axonal transport. The results indicated that both LiCl and MB prevented DFP-induced impairments in anterograde and retrograde axonal transport velocities in a concentration dependent manner. While in vivo studies will be required to confirm our in vitro findings, these experiments support the potential of LiCl and MB as repurposed drugs for the treatment of the long-term neurological deficits associated with OP exposure (currently an unmet medical need).

Corresponding Author: Alvin V. Terry Jr., Ph.D., Department of Pharmacology & Toxicology, 1120 15th Street, CB-3545, Augusta University, Augusta, Georgia 30912, Phone: 706-721-9462, Fax: 706-721-2347, aterry@augusta.edu.

Declaration of interests

The authors declare that they have no known competing financial interests or personal relationships that could have appeared to influence the work reported in this paper.

Keywords

Nerve Agent; Pesticide; Organophosphate; Gulf War Illness; Phenotypic Screening; Drug Repurposing

1. Introduction

The highly toxic class of chemicals known as the organophosphates have valuable uses worldwide especially as pesticides and insecticides in agriculture and for controlling deadly vector-borne illnesses (for reviews see Cooper and Dobson, 2007; Fernandez-Cornejo et al., 2014). In recent years, the widespread use of OPs has become controversial, however, since they have been linked to a variety of deleterious health effects in humans including long-term neurological impairments such as those observed in syndromes like Gulf War Illness (reviewed, Naughton and Terry, 2018). Moreover, the intentional use of chemical warfare agents (CWAs) by rogue governments and terrorist organizations continues to represent a threat worldwide and OPs such as sarin and soman are among the most toxic CWA used (Worek et al., 2016).

Antidotal treatment regimens (pralidoxime, atropine, and benzodiazepines) are available to combat the symptoms of acute OP toxicity, which result from the irreversible inhibition of acetylcholinesterase-AChE. However, there are no established treatments for the neurological impairments that have been identified as long-term consequences of acute OP toxicity or repeated exposures to lower levels of OPs that were not associated with symptoms of acute toxicity. A barrier to the formulation of new treatment strategies in this context is the lack of knowledge regarding the underlying mechanisms of the neurological impairments.

In addition to AChE, OPs can affect hundreds of other enzymes, receptors, and proteins (Costa 2018) and influence multiple neurobiological processes including inflammation (Koo et al., 2018; Mohammadzadeh et al., 2018), oxidative stress (Eftekhari et al., 2018; Abolaji et al., 2017), autoimmunity (Abou-Donia et al., 2013, 2017; El Rahman et al., 2018), and axonal transport (Gao et al., 2016, 2017). Given this level of complexity, it would appear that a multi-target approach to drug discovery would likely have more potential for treating long-term OP toxicity than a single-target single drug approach. However, there must be some rationale for narrowing down the host of potential drug targets. Given the fundamental nature of axonal transport to neuronal health and its impairment in multiple neurologic and neurodegenerative illnesses, we rationalized that this process might serve as a general focus area for novel therapeutic strategies against OP toxicity. Notably, axonal transport is essential for the movement of important macromolecules (e.g., proteins, lipids, mRNA, mitochondria) to and from a neuron’s cell body and impairments in axonal transport have been implicated in multiple neurological illnesses including amyotrophic lateral sclerosis, Alzheimer’s disease, Huntington’s disease, Parkinson’s disease, Pick’s disease, and progressive supranuclear palsy (see Millecamps and Julien, 2013 for review). It is noteworthy that many of these illnesses are characterized by similar neurological and

neurobehavioral deficits that have been observed in people who have been exposed to OP-based pesticides (reviewed, Naughton and Terry, 2018).

Deficits in axonal transport resulting from OP exposure were first demonstrated in an ex vivo rat optic nerve preparation by Reichart and Abou-Dorin (1980) where relatively high doses of OPs (i.e., phenylphosphonothioate esters and TOCP) impaired fast anterograde axonal transport. We have subsequently observed impairments in axonal transport in multiple model systems (at relatively low concentrations or doses) including ex vivo sciatic nerve preparations (ex vivo) (Terry et al., 2007), cultured neurons (in vitro) (Gao et al., 2016; 2017), and living rats (in vivo) using manganese-enhanced magnetic resonance imaging (Hernandez et al., 2015; Naughton et al., 2018). Experimental efforts to identify potential underlying mechanisms of the OP-related impairments in axonal transport in our laboratory and others have resulted in observations of kinesin detachments after OP exposures (Gearhart et al., 2007), disruptions in mitochondrial trafficking and morphology (Middlemore-Risher et al., 2011), and decreases in microtubule outgrowth and tubulin acetylation (Rao et al., 2017; Yang et al., 2018). These observations highlight potential therapeutic targets.

It is also important to note that, while the worldwide population of individuals suffering long-term neurological consequences of OP exposures may be significant, it is unlikely that major pharmaceutical companies will invest in large-scale drug discovery efforts for this indication given the relatively small market. Accordingly, it is of interest to evaluate compounds that are already FDA approved for other indications against the negative effects of OPs on axonal transport. Therefore, as will be evident below, in the experiments described in this report, we employed a multi-target, phenotypic screening and drug repurposing strategy (see review, Medina-Franco et al., 2013) for the evaluations of potential novel OP-treatments.

Phenotypic drug screening is based on evaluations of functional outcomes resulting from drug treatments (e.g., effects on axonal transport velocity) as opposed to engagement of a specific molecular target. This strategy provides the benefit of screening multiple drugs with different mechanisms of action within the same assay. Phenotypic screening has gained renewed interest in recent years in drug discovery after numerous clinical failures of drugs identified through target-driven high throughput screening (Vincent et al., 2015). Our phenotypic drug screening studies were performed using a primary neuronal culture model and time-lapse live imaging microscopy. Two multi-target compounds, lithium chloride (LiCl) and methylene blue (MB), which are FDA approved for the treatment of non-OP related disorders, (Bipolar disorder and methhemeglobinemia, respectively) were selected for screening in our live imaging assay. LiCl was chosen in part based on previous reports of its ability to increase axonal transport rates in other model systems (Decker et al., 2010; Flores III et al., 2011), while MB was selected for its ability to improve mitochondrial function and provide neuroprotection in multiple models (see further details in the Discussion). We chose to evaluate these compounds against the negative effects of the OP, diisopropylfluorophosphate (DFP) on axonal transport. DFP is an alkyl phosphorofluoridate that is often used as a surrogate nerve agent in laboratory studies since it possesses a great

deal of structural homology with other highly toxic nerve agents such as sarin and soman, but is less potent (Hobbiger, 1972) and less dangerous for laboratory personnel.

2. Materials and Methods

2.1 Chemicals and Reagents

Diisopropylfluorophosphate (DFP) and Methylene Blue were purchased from Sigma Aldrich (St. Louis, MO). Lithium chloride was purchased from Fluka/Honeywell (Charlotte, NC). All primary antibodies were purchased from Cell Signaling Technologies (Danvers, MA) and secondary antibodies were purchased from Jackson ImmunoResearch Laboratories (West Grove, PA). Cell culture reagents were purchased from Fisher Scientific (Pittsburgh, PA) unless otherwise stated.

2.2 Cell Culture

Primary cortical neurons were prepared as previously described (Gao et al., 2016; 2017) with minor changes. Briefly, embryos were harvested from Sprague-Dawley pregnant dams at gestation day E18. Embryonic Cortices were carefully dissected, then incubated at 37°C for 15min in 0.25% Trypsin (Life Technologies, Carlsbad, CA) in the presence of DNAse (Sigma #D4513), with gentle agitation every 5 min. Tissue was then briefly rinsed in HBSS, followed by trituration with a glass fire-polished pasture pipette in neurobasal media (Gibco, Gaithersburg, MD) with 2% B27 and 10% FBS in the presence of DNAse. Dissociated cells were then centrifuged for 8min at 25°C at 200G. Pelleted cells were then re-suspended in neurobasal media with 2%B27, 10%FBS, and 100U/mL penicillin-streptomycin (Life Technologies, Grand Island, NY) and plated at a density of 500,000 cells/mL. Plating media was replaced with serum-free media (neurobasal media with 2%B27, 100U/mL penicillin-streptomycin and 0.5mM Glutamax) after 2hrs. Media was changed every 4 days with 0.5μM ARAC added overnight on DIV3 and penicillin-streptomycin removed before transfection. Cells were maintained at 37°C with 5% CO_2 in a cell culture incubator.

2.3 Transfection and Drug Treatment

The method used in this study to measure axonal transport was a modification of our previously published studies where time-lapse microscopy techniques were employed to measure the trafficking of membrane-bound organelles (MBOs) containing a transfected fluorophore-tagged amyloid precursor protein (APP) cDNA construct. Importantly, APP is well documented to travel in neurons by fast axonal transport (see further details in Gao et al., 2016). Cells were transfected on DIV5–6 with pEGFP-n1-APP (Addgene #69924). Briefly, 2μg cDNA was incubated at room temperature in 25μl Neurobasal Media, separately 2 μL Lipofectamine® 2000 (Thermo Fisher) was incubated in 25uL Neurobasal Media. After 5 min the two mixtures were combined and incubated at room temperature for an additional 20min, before being added to the culture dish. Treatments with 1.0 nM DFP or Vehicle (ultrapure water) were added to the culture dish for 24hrs, 4–6 hours after transfection on DIV5–6. The concentration of DFP (1.0 nM) used in the experiments and the exposure time (24 hrs) described in this report was selected from our previously published studies (Gao et al., 2016) since it was associated with impairments of anterograde and retrograde axonal transport, was not associated with overt cell toxicity, and was not

associated with significant AChE inhibition. We previously observed that DFP impaired anterograde and retrograde axonal transport both after 1 hour and 24 hours of exposure, however, the magnitude of the effect was somewhat higher after 24 hrs (particularly at the selected 10 nM concentration), so this DFP exposure period was selected for evaluations of potential treatments.

For Lithium chloride evaluations, cells were treated with 1.0 nM DFP for 24hrs, with LiCl (01μM-10mM) or vehicle (ultrapure water) added during the final 2hrs before live imaging (22hrs after addition of DFP). The culture incubation time (2 hours) and concentrations of LiCl were selected based on previously published reports where LiCl was shown to increase axonal transport velocities in cultured neurons in toxin (Aβ) and molecular (DISC1 knockdown) models (Decker et al., 2010; Flores III et al., 2011). For Methylene blue evaluations, (0.1–100nM) methylene blue or vehicle (ultrapure water) was co-incubated with 1.0 nM DFP for 24hrs. The 24 hr incubation time and concentrations of MB were selected based on their ability to improve the viability of cultured cells exposed to neurotoxins (e.g., rotenone, antimycin A) and increase ATP production (Wen et al., 2011).

2.4 Live Imaging and Analysis

Live imaging was performed as described previously (Gao et al., 2016; 2017). Briefly, coverslips were placed in a live imaging chamber and media was changed to clear Neurobasal media immediately before imaging. All experiments were performed on a Zeis LSM780 inverted confocal microscope, equipped with an environmental chamber maintained at 37°C with 5% CO_2. All experiments were performed 24–36hrs after transfection. GFP-APP transfected neurons were located in primary cortical cultures under 63X magnification (1.42 numerical aperture) and axons were identified by their fluorescence and morphological features as originally described by Kriegstein and Dichter (finest, longest cell processes with no spines) (Kriegstein and Dichter, 1983). Axons were video recorded for 3 min and frames were captured at a rate of one frame every 2 sec for a total of 90 frames (Zen, Carl Zeiss) to track the movements of dynamic particles and identify stationary particles. All image processing and analysis was performed using FIJI/ImageJ 1.52b. Images were processed using the bleach correction tool and axons were straightened using the “straighten curved objects” plugin. Kymographs were manually generated using the “Kymograph Action Tool” plugin and analyzed using the KymoAnlyzer plugin toolkit V1.01 (Neumann et al., 2017). The following settings were adjusted in KymoAnalyzer: Cmin=3, cminRV=3, pixel size =0.307, frame rate=0.5, factor=0.33/frame. Anterograde cargos were defined as cargos that moved more than 3μm away from the cell body, retrograde cargos were defined as having moved more than 3μm towards the cell body, reversing cargos were defined as having changed directions and traveled more than 3μm, stationary cargos were defined as having traveled less than 3μm. A pause was defined as period where a cargo’s speed was temporarily reduced to ≤0.15μm/s. Density was calculated as the total number of cargos (anterograde, retrograde, stationary, and reversing) per micron of axon length. Net velocities were calculated based on the total distance traveled during each 3 minute video, including time spent pausing or reversing directions. Fig 1 provides an example of a GFP-APP transfected neuron, a representative kymograph, and a series of video frames indicating

movements of individual membrane-bound organelles (MBOs) in the anterograde or retrograde direction.

2.5 Cell Lysates

Cells were grown in 6-well plates at a density of 500,000 cells/mL for 6 days in vitro then treated for 24hrs with 1nM DFP prior to processing. Each plate was rinsed twice using ice cold PBS, cells were then scraped in 200uL 1X RIPA buffer containing the following inhibitors: Phosphatase cocktail 2 (Sigma #P5726), Phosphatase inhibitor cocktail 3 (Sigma #P0044) protease inhibitor cocktail (Sigma #P8340), 10mM sodium fluoride, and 1mM PMSF. Treated cells from each six well plate were pooled such that 1 plate = 1 independent experiment (n=4). Scraped cells were then centrifuged at 16,000g, 4°C for 20min, the supernatant was then removed and stored at −80°C until further processing.

2.6 Immunoblotting and Analysis

Immunoblotting was performed using standard techniques. Briefly, samples were run on 12% gels at 50–100V. Samples were then transferred overnight at 30V onto a PVDF membrane (Immobilon®-P, Millipore). The membrane was incubated for 1hr in 0.2% I-block reagent (Applied Biosystems), then incubated in 1:250 primary P-GSK antibody (cell signaling technologies #9336) over night at 4°C with gentle agitation. The Membrane was then rinsed 3 times with TTBS before incubation with 1:5000 secondary antibody (Jackson ImmunoResearch labs #111–035-003) for 1hr at RT. The membrane was then rinsed 3 times in TTBS and incubated for 5min in ECL (Western Lighting® ECL Pro, PerkinElmer) before being imaged using a G Box chemiluminescent imaging system (Syngene). The Membrane was then stripped via 20min incubation at 37°C with gentle agitation using Restore™ Western Blot Stripping Buffer (Fisher Scientific). The membrane was then rinsed 3 times in TTBS. The membrane was then probed and imaged again using similar procedures as described above, with 1:1000 GSK primary antibody (cell signaling technologies #9315) and 1:10,000 secondary antibody (Jackson ImmunoResearch labs #111–035-003). Densitometry was performed in FIJI/ImageJ with P-GSK normalized to total GSK.

2.7 Statistics

Statistical analysis was performed using SigmaPlot 11.2 and statistical significance was assessed using an alpha level of 0.05. Student t tests and analysis of variance were used as appropriate followed by the Student Newman Keuls test for post hoc analysis after ANOVA comparisons. All results are expressed as the mean (±SEM).

3. Results

3.1 GFP-APP transfection and live imaging

Twenty-four hours following transfection, cultured neurons exhibited clear expression of GFP-APP in the soma and axons (Fig 1A). For imaging, individual GFP-APP -labeled MBO’s in axons were identified as distinct (green fluorescent) structures with a circular or tubular shaped appearance (see the arrows in Figure 1A). Definitive proximal and distal axonal regions of each axon were identified and corresponding kymographs (see Fig 1B for a sample) demonstrate that many MBOs were highly mobile, moving in both the anterograde

and retrograde directions, while others remained stationary. The arrows in Fig 1C indicate individual MBOs moving along the axon at various stages in the anterograde and retrograde direction.

3.2 Axonal Transport Velocity

The velocity of GFP-APP labeled MBO movements in cortical axons observed in this study under control conditions, ~0.4–2.0 μm/sec in the anterograde, and ~0.4–1.5 μm/sec in retrograde direction, is similar to that observed in our previously published studies using APPDendra2-labeled MBOs (Gao et al., 2016; 2017). Moreover, the range of velocities generally fits within the range (0.5–3.0μm/sec) that is considered as “fast axonal transport” (see review, Maday et al., 2014).

3.3 DFP Disrupts Axonal Transport

Following 24hr incubation with 1.0 nM DFP we observed significant decreases in the anterograde and retrograde velocities of GFP-APP containing membrane-bound organelles (MBOs) (Figures 2 and 3) similar to the decreases described in our previous report where APPDendra2-labeled MBOs were analyzed. (Gao et al., 2016). While some modest changes were observed, we did not detect any statistically significant differences in the percentage of particles moving in the anterograde or retrograde directions nor did we detect significant changes in the percentage of stationary or reversing particles. We also analyzed the total density (cargos per μm) of particles and found no significant differences in the density of cargos after DFP exposure. DFP treatment was also not associated with significant changes in pause duration. An increase in pause frequency was observed after DFP exposure; however, this effect was only significant in one of the two data sets presented (Table 1).

3.4 Lithium Chloride

The effects of DFP on axonal transport were attenuated by co-incubation with LiCl in a concentration dependent manner. Interestingly, we observed an inverted U shaped concentration-response curve indicating that lower concentrations (10μM-1mM) of lithium were most effective in preventing DFP-induced anterograde axonal transport deficits while higher concentrations (1mM-10mM) were associated with reductions in velocity (Figure 2). With respect to retrograde velocities, a similar inverted U trend was observed, however only treatment with 100μM LiCl significantly prevented DFP-induced deficits (Figure 2). Treatment with 100μM LiCl alone was not associated with significant changes in velocity when compared to vehicle. We did not observe significant changes in the percentage of cargos traveling in the anterograde or retrograde direction, remaining stationary, or reversing after co-incubation of LiCl with DFP. Interestingly, 100μM LiCl alone was associated with a significant decrease in the percentage of stationary particles when compared to DFP. While the majority of LiCl concentrations tested were not associated with significant changes in cargo density, the lowest concentration (1μM) was associated with a significantly higher density compared to DFP, while the highest concentration (10mM) of LiCl was associated with a significantly lower density compared to DFP. Lithium treatment was not associated with significant changes in pause duration or pause frequency. Interestingly, 100μM LiCl was associated with an increased pause frequency compared to vehicle alone (Tables 1 and 2).

3.5 Methylene Blue

24hr co-incubation of MB with DFP was also associated with concentration dependent increases in the velocity of GFP-APP containing MBOs. MB significantly enhanced anterograde axonal transport velocities across a range of concentrations (1nM-100nM), while only 10nM was associated with significantly increased retrograde velocities (Figure 3). The majority of the concentrations of MB were not associated with significant changes in the percentage of anterograde, retrograde, stationary, or reversing cargos. However, 10nM MB treatment was associated with a significant decrease in the number of stationary particles compared to 1nM DFP. Additionally, Vehicle+ 10nM MB was associated with a significant increase in the percentage of particles moving in the anterograde direction and a significant decrease in the number of stationary particles compared to 1nM DFP. None of the treatments were associated with significant changes in the number of cargos per micron (density). With respect to pause duration, we did not observe significant changes in response to any treatment. However, 0.1nM MB treatment was associated with a significantly higher pause frequency compared to DFP, while the remaining concentrations tested did not significantly affect pause frequency (Tables 1 and 2).

3.6 GSK Phosphorylation in vitro

Some previous studies have indicated that OPs such as omethalate and chlorpyrifos can alter the phosphorylation of GSK (Qiao et al., 2017; Chen et al., 2012) (see additional details in the Discussion). Thus, in order to determine if changes in the phosphorylation status of GSKIIIβ might be responsible for DFP induced axonal transport deficits, we probed for changes in the phosphorylation of GSKIIIβ at the ser9 phosphorylation site after exposure to 1nM DFP for 24hrs in cultured primary cortical neurons. Surprisingly, western blot analysis revealed no significant changes in the phosphorylation of GSKIIIβ after exposure to DFP (Figure 4), indicating that it is unlikely to be a mechanistic factor in the DFP-induced reduction of axonal transport velocity (i.e., at this particular concentration). Furthermore, the concentrations of LiCl that were most effective in preventing DFP-induced deficits in axonal transport velocity fell below the threshold for GSK inhibition (see Discussion), while those that were associated with slower transport rates (right side of the inverted U dose-response curve), fell within the known threshold for GSK inhibition by LiCl (Klein and Melton, 1996).

4. Discussion

4.1 DFP Inhibits Axonal Transport

In the currently study, our first observation was that 24hr exposure to 1nM DFP was associated with decreases in anterograde and retrograde transport velocity of fluorescent, amyloid precursor protein (APP) containing MBOs (Figures 2 and 3) as we have previously reported (Gao et al., 2016). We observed only modest, non-significant changes in the percentage of MBOs moving in the anterograde and retrograde direction or the percentages of stationary cargos in association with DFP exposure. In our previously published experiments (Gao et al., 2016) we observed small, but statistically significant decreases in the percentage of MBOs moving in the anterograde direction and a small increase in the percentages of stationary cargos in association with the 1.0 nM DFP concentration (Table 1).

Similar to the current study, we did not observe any DFP-related changes in the percentage of MBOs moving in the retrograde direction in the Gao et al., 2016 study. These observations appear to suggest that while the 1.0 nM concentration of DFP can clearly impair anterograde and retrograde axonal transport velocities, it is on the threshold for affecting the percentages of cargoes moving in a particular direction or remaining stationary. An additional observation in the current study was that no significant differences were present in the overall density of cargos after DFP treatment, indicating that the observed axonal transport deficits likely occurred independently of alterations in APP synthesis or its packaging in vesicles. DFP treatment was also not associated with significant changes in pause duration, indicating that prolonged pausing of cargos is not a contributing factor to reduced axonal transport velocities. An increase in pause frequency was observed after DFP exposure; however, this effect only reached significance in one of the two data sets collected (Table 1). Thus, increases in pause frequency may contribute to the slower transport rates observed, but this observation requires additional replication before it could be viewed as a definitive finding.

4.2 Lithium Chloride Reverses DFP-induced Axonal Transport Deficits in vitro.

Our next observation was that LiCl prevented the negative effects of DFP in a concentration dependent manner (Figure 2). Both anterograde and retrograde velocities were improved following LiCl treatment and the concentration response curve followed an inverted U shaped pattern, indicating that an optimal concentration range is required to achieve full efficacy. LiCl was not associated with significant changes in the percentage of anterograde, retrograde, stationary, or reversing cargos (Table 1). Interestingly, we did observe a significant decrease in stationary cargos when comparing Veh+LiCl 100μM to 1nM DFP. This indicates that lithium treatment alone may have some modest effects on the overall percentage of particles moving. Another interesting observation was that the, the lowest (1μM) and highest (10mM) concentrations of LiCl (when combined with DFP) were associated with modest, but statistically significant changes in the overall density of cargos (i.e., increased and decreased, respectively) while the remaining concentrations had no effect. These observations may indicate that specific combinations of DFP and LiCl concentrations may have the potential to induce minor changes in APP expression. Minor changes in pause duration and frequency were also observed with LiCl treatment particularly at concentrations associated with faster axonal transport speeds; however, these changes were not statistically significant. Surprisingly, Veh+100μM LiCl was associated with a significant increase in pause frequency when compared to 1nM DFP treatment. This observation appears paradoxical since this treatment was not associated with increases in pause frequency when co-incubated with DFP (Table 1).

4.3 Methylene Blue Prevents DFP-induced Axonal Transport Deficits in vitro.

Methylene blue (MB) was also effective against DFP induced axonal transport deficits in a concentration dependent manner increasing velocity of both anterograde and retrograde MBOs (Figure 3). Veh+10nM MB did not significantly affect axonal transport velocities when compared to vehicle controls. The majority of MB concentrations tested did not have significant effects on the percentage of anterograde, retrograde, stationary, or reversing cargos. However, 10nM MB treatment was associated with a significant decrease in the

percentage of stationary cargos when compared to 1nM DFP. This result may be indicative of overall changes in transport dynamics stimulated by MB (Table 1). Additionally, Veh +10nM MB was associated with a significant decrease in the percentage of stationary cargos and a significant increase in the percentage of anterograde cargos compared to 1nM DFP. These results may indicate that MB possesses the ability to stimulate generalized changes in the movement dynamics of APP-bound cargos. No significant changes were detected in cargo density across any concentration of MB tested, indicating that its effects (similar to Lithium Chloride) are likely to occur independently of gross changes in APP synthesis or its packaging in vesicles. MB treatment was also not associated with significant changes in pause duration indicating that reductions in the pause time of individual cargos is not a contributing factor to the effects of MB on axonal transport (Table 2). Finally, with the exception of the 0.1 nM concentration of MB (which was associated with an increase in pause frequency when combined with DFP), the majority of MB concentrations tested did not affect pause frequency, when compared to 1nM DFP alone (Table 1). The basis for this observation is unclear.

While the specific mechanisms of the positive effects of LiCl and MB on axonal transport were not the primary focus of the current study, each compound has a number of potentially relevant pharmacological actions. LiCl has been used in the treatment of Bipolar Disorder dating back to the mid-20th century and it has been the focus of numerous pharmacological studies. The best characterized pharmacological effects of lithium pertain to its inhibition of GSKIII, both through direct inhibition by competitively binding to the Mg+ binding site, as well as indirect inhibition through an increase in phosphorylation of the inhibitory site (ser9) (Klein and Melton, 1996; Pan et al., 2011). Previously published reports have demonstrated that 1mM LiCl does not inhibit GSK, while 10mM LiCl strongly inhibits GSK (Klein and Melton, 1996). Thus, in our study, the effective range of LiCl concentrations fell below the threshold for GSK inhibition, while doses that were within the range of effective GSK inhibition were associated with deleterious effects on axonal transport. These observations led us to conclude that the positive effects of LiCl on axonal transport velocities are not likely to be mediated by GSKIIIβ inhibition. Such findings are not unprecedented, as previous reports have shown LiCl induced increases in axonal transport speed that could not be mimicked by specific inhibitors of GSK or GSK knockdown by shRNA (Flores III et al., 2011). GSKIIIβ acts as a negative regulator of axonal transport and phosphorylation of GSKIIIβ at serine 9 has been associated with its inhibition, thus we initially expected to observe decreased phosphorylation of GSKIIIβ after DFP exposure. Interestingly, we did not observe significant changes in the level of pGSK after exposure to DFP (Figure 4). These findings are in contrast to Qiao and colleagues who demonstrated decreased GSK phosphorylation after exposure to the OP omethalate (Qiao et al., 2017) and Chen and colleagues who observed hyperphosphorylation of GSK after exposure to the OP chlorpyrifos (Chen et al., 2012). Lithium has been shown to stabilize microtubules (Bhattacharyya and Wolf, 1976) within the range of concentrations that we found effective at preventing the negative effects of DFP on axonal transport. This may represent a potential mechanism of the positive effects of LiCl in our experiments, given that OPs have been shown to reduce tubulin acetylation, (Rao et al., 2017; Yang et al., 2018) a post translational modification typically associated with reduced microtubule stability. Additionally, OPs have

been shown to prevent tubulin polymerization and covalently modify tubulin (Prendergast et al., 2007; Grigoryan et al., 2008). Lithium treatment has also been shown to upregulate a number of transport and cytoskeletal related proteins including kinesin-1 heavy chain (Gottschalk et al., 2017). A recent study found that Lithium treatment is also associated with increased activity of the cytoskeletal modulator Collapsin Response Mediator Protein-2 (CRMP2) through both GSK-dependent and independent pathways (Tobe et al., 2017). CRMP2 is an important cytoskeletal regulator that is involved with axonal transport (Arimura et al., 2009; Kimura et al., 2005; Kawano et al., 2005), as well as microtubule assembly (Fukata et al., 2002). Thus, lithium induced modulation of CRMP2 activity through GSK-independent pathways may provide a rational explanation for the observed effects of LiCl either through the activity of CRMP2 as a cargo receptor or through its activity in promoting microtubule assembly. Finally, axonal transport is regulated by a number of additional kinases beyond GSK such as PKC, AKT, ERK1/2, cdk5, JNK and p38 kinase (Gibbs et al., 2015) all of which can be effected by lithium treatment (Chen et al., 2003; Pardo et al., 2003; Jorda et al., 2005; Pan et al., 2011; Valvassori et al., 2017).

MB is a tricyclic phenothiazine that was the first fully synthetic drug to be used in a therapeutic context (Schirmer et al., 2011). For our studies, the positive effects of MB on mitochondrial respiration and ATP production (Wen et al., 2011) were major factors in our choice of this compound as a potential OP-treatment. Previous studies have shown that the OPs CPF and CPO can produce disruptions in mitochondrial morphology and transport (Middlemore-Risher et al., 2011). Interestingly, exogenous ATP application has been shown to increase the velocity of kinesin moving along microtubules in a model system in a concentration dependent manner (Schnitzer and Block, 1997). Additional studies have shown increases in axonal transport by leveraging energy production through the application of fatty acids and by the application of extracellular ATP (Takenaka et al., 2003; Sakama et al., 2003). A similar strategy has been demonstrated in the field of exercise science and muscle physiology, in which creatine supplementation can be used to enhance muscle performance (Casey and Greenhaff, 2000). By donating a phosphate molecule, creatine phosphate (CP) catalyzes the conversation of ADP to ATP and provides ATP to power myosin driven muscle contraction (Widmaier et al., 2007). Given that myosin is a molecular motor ATPase similar to dynein and kinesin, it is possible that similar strategies to increase the available supply of ATP may increase their rate of movement. An alternate explanation for the observed effect of MB is that increased ATP levels may lead to a higher rate of microtubule polymerization. ATP has been shown to promote tubulin polymerization (Zabrecky and Cole, 1982) and may counterbalance previously observed disruptions in tubulin polymerization after OP exposure (Prendergast et al., 2007). Interestingly, MB has also been shown to inhibit GSK through increased phosphorylation at ser9 -site and decreased phosphorylation at the tyr216-site (Chen et al., 2019). While we did not observe changes in GSK phosphorylation following DFP exposure, we cannot rule out the possibility that MB may have increased axonal transport velocities through a compensational mechanism involving decreased GSK activity.

4.4 Phenotypic screening assay and Multifunctional Drugs for the treatment of Organophosphate Toxicity

As discussed in the Introduction, axonal transport can be regulated by a number of different factors such as signaling kinases; post-translational modifications of microtubules and microtubule associated proteins, as well as mitochondrial activity. Thus, a target driven screen focused solely on one particular mechanism may not be the most fruitful approach. Phenotypic drug screening assays provide the benefit of applying an unbiased target and agnostic approach to drug discovery. In fact, an analysis by Swinney and Anthony found that from 1999–2008 the majority of new first in class drugs were discovered using phenotypic screening, despite a strong inclination towards target-driven approaches during that time (Swinney and Anthony 2011). Given the high cost of drug development and the relatively small population of patients affected by OP exposure, we reasoned that the repurposing of currently FDA approved drugs might provide the most reasonable path towards providing treatment for such patients. We thus selected candidate compounds for screening that had already been FDA approved for other therapeutic uses. We chose to evaluate two different drugs for their potential ability to reverse OP-induced axonal transport deficits. However, axonal transport deficits are not the only detrimental effects associated with OP exposure. Thus, when choosing potential therapeutic compounds to evaluate, drugs with multifunctional and multi-target properties were chosen. MB has a number of beneficial effects, which may be of therapeutic value after OP exposure. Mitochondria are a primary site of action by MB, and show disrupted transport and morphology after OP exposure (Middlemore-Risher et al., 2011). Additionally the autophagy stimulating properties of MB (Congdon et al., 2012) may be of particular benefit. A recent report has shown that exposure to the OP chlorpyrifos-oxon (CPO) can cause tubulin to form intermolecular cross-links leading to high molecular weight tubulin aggregates, similar to the aggregation of various proteins in neurodegenerative disorders (Schopfer and Lockridge, 2018). Autophagic clearance of such aggregations could be of therapeutic value. MB has also been shown to have antioxidant and anti-inflammatory properties (Tucker et al., 2018) and OP exposure has been linked to increases in oxidative stress and inflammation (Eftekhari et al., 2018; Abolaji et al., 2017; Koo et al., 2018; Mohammadzadeh et al., 2018). Furthermore, MB has been shown to be neuroprotective in preclinical models of a number of neurodegenerative disorders (Tucker et al., 2018). These properties make MB a good candidate generalized neuroprotection in the treatment of OP related toxicity.

Lithium shares several of the multifunctional properties of MB, such as the ability to induce autophagy (Kerr et al., 2018) and antioxidant properties (Won and Kim, 2017; Kerr et al., 2018). Additionally, lithium has been demonstrated to increase grey matter volumes and white matter integrity (Won and Kim, 2017) as well as to promote re-myelination (Fang et al., 2016). These properties make lithium a good potential candidate in the treatment of Gulf War Illness (GWI), which is characterized by constellation of chronic health symptoms, observed in many United States (US) veterans who served in the 1990–1991 Persian Gulf War. Both grey and white matter have been shown to be decreased in GWI and OP exposure is believed to be a contributing factor to the neurologic symptoms (Chao et al., 2010, 2011; Rayhan et al., 2013; Rosenzweig et al., 2012). Additionally, LiCl has been shown to be effective in reversing depressive behaviors in mice after exposure to the OP omethalate

(Qiao et al., 2017). A recent study by Greenwood and colleagues demonstrated that concentrations of lithium in the high nanomolar to low micromolar range exhibit neuroprotective properties through disruption of the $p75^{NTR}$-Sortilin complex and its internalization (Greenwood et al., 2018). Lithium has also been shown to up-regulate brain derived neurotrophic factor (BDNF) (Won et al., 2017), a neurotrophin well known for its positive role in synaptic plasticity, neuroprotection, and cognitive function.

In summary, the results of the in vitro experiments described in this report indicate that LiCl and MB are effective at attenuating OP-induced axonal transport deficits. The specific culture conditions we chose (LiCl applied during the last 2 hrs of a 24 hr DFP exposure period and MB applied simultaneously with DFP for the entire 24 hr exposure period) support LiCl as a potential antidotal (post toxin exposure) treatment and MB as a prophylactic or preventative approach. Accordingly, these compounds may have potential as repurposed drugs for the treatment/prevention of neurologic symptoms associated with OP exposure. Additional studies will be required to determine if treatment with LiCl and MB can reverse learning and memory deficits and other long-term neurological deficits associated with OP exposure in vivo.

Acknowledgments

The authors would like to thank Ms. Ashley Davis for her administrative assistance in preparing this article. This work was supported by the Congressionally Directed Medical Research Programs (CDMRP), specifically, the Gulf War Illness Research Program (GWIRP), grant number W81XWH-12–1-0536 (Terry) and the National Institutes of Health (NIH) grant GM118915 (Wu).

References

Abolaji AO, Ojo M, Afolabi TT, Arowoogun MD, Nwawolor D, & Farombi EO (2017). Protective properties of 6-gingerol-rich fraction from Zingiber officinale (Ginger) on chlorpyrifos-induced oxidative damage and inflammation in the brain, ovary and uterus of rats. Chem Biol Interact, 270, 15–23. doi:10.1016/j.cbi.2017.03.017 [PubMed: 28373059]

Abou-Donia MB, Abou-Donia MM, ElMasry EM, Monro JA, & Mulder MF (2013). Autoantibodies to nervous system-specific proteins are elevated in sera of flight crew members: biomarkers for nervous system injury. J Toxicol Environ Health A, 76(6), 363–380. doi:10.1080/15287394.2013.765369 [PubMed: 23557235]

Abou-Donia MB, Conboy LA, Kokkotou E, Jacobson E, Elmasry EM, Elkafrawy P, . . . Sullivan, K. (2017). Screening for novel central nervous system biomarkers in veterans with Gulf War Illness. Neurotoxicol Teratol, 61, 36–46. doi:10.1016/j.ntt.2017.03.002 [PubMed: 28286177]

Arimura N, Kimura T, Nakamuta S, Taya S, Funahashi Y, Hattori A, . . . Kaibuchi K (2009). Anterograde transport of TrkB in axons is mediated by direct interaction with Slp1 and Rab27. Dev Cell, 16(5), 675–686. doi:10.1016/j.devcel.2009.03.005 [PubMed: 19460344]

Bhattacharyya B, & Wolff J (1976). Stabilization of microtubules by lithium ion. Biochem Biophys Res Commun, 73(2), 383–390. doi:10.1016/0006-291x(76)90719-1 [PubMed: 826253]

Casey A, & Greenhaff PL (2000). Does dietary creatine supplementation play a role in skeletal muscle metabolism and performance? Am J Clin Nutr, 72(2 Suppl), 607s–617s. doi:10.1093/ajcn/72.2.607S [PubMed: 10919967]

Chao LL, Rothlind JC, Cardenas VA, Meyerhoff DJ, & Weiner MW (2010). Effects of low-level exposure to sarin and cyclosarin during the 1991 Gulf War on brain function and brain structure in US veterans. Neurotoxicology, 31(5), 493–501. doi:10.1016/j.neuro.2010.05.006 [PubMed: 20580739]

Chao LL, Abadjian L, Hlavin J, Meyerhoff DJ, & Weiner MW (2011). Effects of low-level sarin and cyclosarin exposure and Gulf War Illness on brain structure and function: a study at 4T. Neurotoxicology, 32(6), 814–822. doi:10.1016/j.neuro.2011.06.006 [PubMed: 21741405]

Chen C, Zhou F, Zeng L, Jiang Z, & Hu Z (2019). Methylene blue offers neuroprotection after intracerebral hemorrhage in rats through the PI3K/Akt/GSK3beta signaling pathway. J Cell Physiol, 234(4), 5304–5318. doi:10.1002/jcp.27339 [PubMed: 30216439]

Chen RW, Qin ZH, Ren M, Kanai H, Chalecka-Franaszek E, Leeds P, & Chuang DM (2003). Regulation of c-Jun N-terminal kinase, p38 kinase and AP-1 DNA binding in cultured brain neurons: roles in glutamate excitotoxicity and lithium neuroprotection. J Neurochem, 84(3), 566–575. doi:10.1046/j.1471-4159.2003.01548.x [PubMed: 12558976]

Chen WQ, Ma H, Bian JM, Zhang YZ, & Li J (2012). Hyper-phosphorylation of GSK-3beta: possible roles in chlorpyrifos-induced behavioral alterations in animal model of depression. Neurosci Lett, 528(2), 148–152. doi:10.1016/j.neulet.2012.08.084 [PubMed: 22985519]

Congdon EE, Wu JW, Myeku N, Figueroa YH, Herman M, Marinec PS, . . . Duff KE (2012). Methylthioninium chloride (methylene blue) induces autophagy and attenuates tauopathy in vitro and in vivo. Autophagy, 8(4), 609–622. doi:10.4161/auto.19048 [PubMed: 22361619]

Cooper J, & Dobson H (2007). The benefits of pesticides to mankind and the environment. Crop Protection, 26(9), 1337–1348. doi:10.1016/j.cropro.2007.03.022

Costa LG (2018). Organophosphorus Compounds at 80: Some Old and New Issues. Toxicol Sci, 162(1), 24–35. doi:10.1093/toxsci/kfx266 [PubMed: 29228398]

Decker H, Lo KY, Unger SM, Ferreira ST, & Silverman MA (2010). Amyloid-beta peptide oligomers disrupt axonal transport through an NMDA receptor-dependent mechanism that is mediated by glycogen synthase kinase 3beta in primary cultured hippocampal neurons. J Neurosci, 30(27), 9166–9171. doi:10.1523/JNEUROSCI.1074-10.2010 [PubMed: 20610750]

Eftekhari A, Ahmadian E, Azami A, Johari-Ahar M, & Eghbal MA (2018). Protective effects of coenzyme Q10 nanoparticles on dichlorvos-induced hepatotoxicity and mitochondrial/lysosomal injury. Environ Toxicol, 33(2), 167–177. doi:10.1002/tox.22505 [PubMed: 29143438]

El Rahman HAA, Salama M, Gad El-Hak SA, El-Harouny MA, ElKafrawy P, Abou-Donia MB. (2018) A Panel of Autoantibodies Against Neural Proteins as Peripheral Biomarker for Pesticide-Induced Neurotoxicity. Neurotox Res. 33(2):316–336. doi: 10.1007/s12640-017-9793-y. [PubMed: 28875469]

Fang XY, Zhang WM, Zhang CF, Wong WM, Li W, Wu W, & Lin JH (2016). Lithium accelerates functional motor recovery by improving remyelination of regenerating axons following ventral root avulsion and reimplantation. Neuroscience, 329, 213–225. doi:10.1016/j.neuroscience.2016.05.010 [PubMed: 27185485]

Fernandez-Cornejo J, Nehring R, Osteen C, Wechsler S, Martin A, Vialou A, & (2014). Pesticide Use in U.S. Agriculture: 21 Selected Crops, 1960–2008.

Flores R 3rd, Hirota Y, Armstrong B, Sawa A, & Tomoda T (2011). DISC1 regulates synaptic vesicle transport via a lithium-sensitive pathway. Neurosci Res, 71(1), 71–77. doi:10.1016/j.neures.2011.05.014 [PubMed: 21664390]

Fukata Y, Itoh TJ, Kimura T, Menager C, Nishimura T, Shiromizu T, . . . Kaibuchi K (2002). CRMP-2 binds to tubulin heterodimers to promote microtubule assembly. Nat Cell Biol, 4(8), 583–591. doi:10.1038/ncb825 [PubMed: 12134159]

Gao J, Naughton SX, Beck WD, Hernandez CM, Wu G, Wei Z, . . . Terry AV Jr (2017). Chlorpyrifos and chlorpyrifos oxon impair the transport of membrane bound organelles in rat cortical axons. Neurotoxicology, 62, 111–123. doi:10.1016/j.neuro.2017.06.003 [PubMed: 28600141]

Gao J, Naughton SX, Wulff H, Singh V, Beck WD, Magrane J, . . . Terry AV Jr (2016). Diisopropylfluorophosphate Impairs the Transport of Membrane-Bound Organelles in Rat Cortical Axons. J Pharmacol Exp Ther, 356(3), 645–655. doi:10.1124/jpet.115.230839 [PubMed: 26718240]

Gearhart DA, Sickles DW, Buccafusco JJ, Prendergast MA, & Terry AV Jr. (2007). Chlorpyrifos, chlorpyrifos-oxon, and diisopropylfluorophosphate inhibit kinesin-dependent microtubule motility. Toxicol Appl Pharmacol, 218(1), 20–29. doi:10.1016/j.taap.2006.10.008 [PubMed: 17123561]

Gibbs KL, Greensmith L, & Schiavo G (2015). Regulation of Axonal Transport by Protein Kinases. Trends Biochem Sci, 40(10), 597–610. doi:10.1016/j.tibs.2015.08.003 [PubMed: 26410600]

Gottschalk MG, Leussis MP, Ruland T, Gjeluci K, Petryshen TL, & Bahn S (2017). Lithium reverses behavioral and axonal transport-related changes associated with ANK3 bipolar disorder gene disruption. Eur Neuropsychopharmacol, 27(3), 274–288. doi:10.1016/j.euroneuro.2017.01.001 [PubMed: 28109561]

Greenwood SG, Montroull L, Volosin M, Scharfman HE, Teng KK, Light M, . . . Friedman WJ (2018). A Novel Neuroprotective Mechanism for Lithium That Prevents Association of the p75(NTR)-Sortilin Receptor Complex and Attenuates proNGF-Induced Neuronal Death In Vitro and In Vivo. eNeuro, 5(1). doi:10.1523/ENEURO.0257-17.2017

Grigoryan H, Schopfer LM, Thompson CM, Terry AV, Masson P, & Lockridge O (2008). Mass spectrometry identifies covalent binding of soman, sarin, chlorpyrifos oxon, diisopropyl fluorophosphate, and FP-biotin to tyrosines on tubulin: a potential mechanism of long term toxicity by organophosphorus agents. Chem Biol Interact, 175(1–3), 180–186. doi:10.1016/j.cbi.2008.04.013 [PubMed: 18502412]

Hernandez CM, Beck WD, Naughton SX, Poddar I, Adam BL, Yanasak N, . . . Terry AV Jr (2015). Repeated exposure to chlorpyrifos leads to prolonged impairments of axonal transport in the living rodent brain. Neurotoxicology, 47, 17–26. doi:10.1016/j.neuro.2015.01.002 [PubMed: 25614231]

Hobbiger F (1972). Chemotherapy in pesticide poisoning. v. 1972.

Jorda EG, Verdaguer E, Canudas AM, Jimenez A, Garcia de Arriba S, Allgaier C, . . . Camins A (2005). Implication of cyclin-dependent kinase 5 in the neuroprotective properties of lithium. Neuroscience, 134(3), 1001–1011. doi:10.1016/j.neuroscience.2005.04.061 [PubMed: 15979805]

Kawano Y, Yoshimura T, Tsuboi D, Kawabata S, Kaneko-Kawano T, Shirataki H, . . . Kaibuchi K (2005). CRMP-2 is involved in kinesin-1-dependent transport of the Sra-1/WAVE1 complex and axon formation. Mol Cell Biol, 25(22), 9920–9935. doi:10.1128/MCB.25.22.9920-9935.2005 [PubMed: 16260607]

Kerr F, Bjedov I, & Sofola-Adesakin O (2018). Molecular Mechanisms of Lithium Action: Switching the Light on Multiple Targets for Dementia Using Animal Models. Front Mol Neurosci, 11, 297. doi:10.3389/fnmol.2018.00297 [PubMed: 30210290]

Kimura T, Watanabe H, Iwamatsu A, & Kaibuchi K (2005). Tubulin and CRMP-2 complex is transported via Kinesin-1. J Neurochem, 93(6), 1371–1382. doi:10.1111/j.1471-4159.2005.03063.x [PubMed: 15935053]

Klein PS, & Melton DA (1996). A molecular mechanism for the effect of lithium on development. Proc Natl Acad Sci U S A, 93(16), 8455–8459. doi:10.1073/pnas.93.16.8455 [PubMed: 8710892]

Koo BB, Michalovicz LT, Calderazzo S, Kelly KA, Sullivan K, Killiany RJ, & O'Callaghan JP (2018). Corticosterone potentiates DFP-induced neuroinflammation and affects high-order diffusion imaging in a rat model of Gulf War Illness. Brain Behav Immun, 67, 42–46. doi:10.1016/j.bbi.2017.08.003 [PubMed: 28782715]

Koo EH, Sisodia SS, Archer DR, Martin LJ, Weidemann A, Beyreuther K, . . . Price DL (1990). Precursor of amyloid protein in Alzheimer disease undergoes fast anterograde axonal transport. Proc Natl Acad Sci U S A, 87(4), 1561–1565. doi:10.1073/pnas.87.4.1561 [PubMed: 1689489]

Kriegstein AR, & Dichter MA (1983). Morphological classification of rat cortical neurons in cell culture. J Neurosci, 3(8), 1634–1647. [PubMed: 6875660]

Maday S, Twelvetrees AE, Moughamian AJ, & Holzbaur EL (2014). Axonal transport: cargo-specific mechanisms of motility and regulation. Neuron, 84(2), 292–309. doi:10.1016/j.neuron.2014.10.019 [PubMed: 25374356]

Medina-Franco JL, Giulianotti MA, Welmaker GS, & Houghten RA (2013). Shifting from the single to the multitarget paradigm in drug discovery. Drug Discov Today, 18(9–10), 495–501. doi:10.1016/j.drudis.2013.01.008 [PubMed: 23340113]

Middlemore-Risher ML, Adam BL, Lambert NA, & Terry AV Jr. (2011). Effects of chlorpyrifos and chlorpyrifos-oxon on the dynamics and movement of mitochondria in rat cortical neurons. J Pharmacol Exp Ther, 339(2), 341–349. doi:10.1124/jpet.111.184762 [PubMed: 21799050]

Millecamps S, & Julien JP (2013). Axonal transport deficits and neurodegenerative diseases. Nat Rev Neurosci, 14(3), 161–176. doi:10.1038/nrn3380 [PubMed: 23361386]

Mohammadzadeh L, Hosseinzadeh H, Abnous K, & Razavi BM (2018). Neuroprotective potential of crocin against malathion-induced motor deficit and neurochemical alterations in rats. Environ Sci Pollut Res Int, 25(5), 4904–4914. doi:10.1007/s11356-017-0842-0 [PubMed: 29204935]

Naughton SX, Hernandez CM, Beck WD, Poddar I, Yanasak N, Lin PC, & Terry AV Jr. (2018). Repeated exposures to diisopropylfluorophosphate result in structural disruptions of myelinated axons and persistent impairments of axonal transport in the brains of rats. Toxicology, 406–407, 92–103. doi:10.1016/j.tox.2018.06.004 [PubMed: 29894704]

Naughton SX, & Terry AV Jr. (2018). Neurotoxicity in acute and repeated organophosphate exposure. Toxicology, 408, 101–112. doi:10.1016/j.tox.2018.08.011 [PubMed: 30144465]

Neumann S, Chassefeyre R, Campbell GE, & Encalada SE (2017). KymoAnalyzer: a software tool for the quantitative analysis of intracellular transport in neurons. Traffic, 18(1), 71–88. doi:10.1111/tra.12456 [PubMed: 27770501]

Pan JQ, Lewis MC, Ketterman JK, Clore EL, Riley M, Richards KR, . . . Haggarty SJ (2011). AKT kinase activity is required for lithium to modulate mood-related behaviors in mice. Neuropsychopharmacology, 36(7), 1397–1411. doi:10.1038/npp.2011.24 [PubMed: 21389981]

Pardo R, Andreolotti AG, Ramos B, Picatoste F, & Claro E (2003). Opposed effects of lithium on the MEK-ERK pathway in neural cells: inhibition in astrocytes and stimulation in neurons by GSK3 independent mechanisms. J Neurochem, 87(2), 417–426. doi:10.1046/j.1471-4159.2003.02015.x [PubMed: 14511119]

Prendergast MA, Self RL, Smith KJ, Ghayoumi L, Mullins MM, Butler TR, . . . Terry AV Jr (2007). Microtubule-associated targets in chlorpyrifos oxon hippocampal neurotoxicity. Neuroscience, 146(1), 330–339. doi:10.1016/j.neuroscience.2007.01.023 [PubMed: 17321052]

Qiao J, Rong L, Wang Z, & Zhang M (2017). Involvement of Akt/GSK3beta/CREB signaling pathway on chronic omethoate induced depressive-like behavior and improvement effects of combined lithium chloride and astaxanthin treatment. Neurosci Lett, 649, 55–61. doi:10.1016/j.neulet.2017.03.048 [PubMed: 28366776]

Rao AN, Patil A, Brodnik ZD, Qiang L, Espana RA, Sullivan KA, . . . Baas PW (2017). Pharmacologically increasing microtubule acetylation corrects stress-exacerbated effects of organophosphates on neurons. Traffic, 18(7), 433–441. doi:10.1111/tra.12489 [PubMed: 28471062]

Rayhan RU, Stevens BW, Timbol CR, Adewuyi O, Walitt B, VanMeter JW, & Baraniuk JN (2013). Increased brain white matter axial diffusivity associated with fatigue, pain and hyperalgesia in Gulf War illness. PLoS One, 8(3), e58493. doi:10.1371/journal.pone.0058493

Reichert BL, & Abou-Donia MB (1980). Inhibition of fast axoplasmic transport by delayed neurotoxic organophosphorus esters: a possible mode of action. Mol Pharmacol, 17(1), 56–60. [PubMed: 6155603]

Rosenzweig I, Bodi I, & Nashef L (2012). Comorbid multiple sclerosis and TDP-43 proteinopathy in a gulf war sea captain. J Neuropsychiatry Clin Neurosci, 24(1), E41–42. doi:10.1176/appi.neuropsych.11030066

Sakama R, Hiruma H, & Kawakami T (2003). Effects of extracellular atp on axonal transport in cultured mouse dorsal root ganglion neurons. Neuroscience, 121(3), 531–535. doi:10.1016/s0306-4522(03)00463-9 [PubMed: 14568014]

Schirmer RH, Adler H, Pickhardt M, & Mandelkow E (2011). “Lest we forget you--methylene blue...”. Neurobiol Aging, 32(12), 2325 e2327–2316. doi:10.1016/j.neurobiolaging.2010.12.012

Schnitzer MJ, & Block SM (1997). Kinesin hydrolyses one ATP per 8-nm step. Nature, 388(6640), 386–390. doi:10.1038/41111 [PubMed: 9237757]

Schopfer LM, & Lockridge O (2018). Chlorpyrifos oxon promotes tubulin aggregation via isopeptide cross-linking between diethoxyphospho-Lys and Glu or Asp: Implications for neurotoxicity. J Biol Chem, 293(35), 13566–13577. doi:10.1074/jbc.RA118.004172 [PubMed: 30006344]

Sisodia SS, Koo EH, Hoffman PN, Perry G, & Price DL (1993). Identification and transport of full-length amyloid precursor proteins in rat peripheral nervous system. J Neurosci, 13(7), 3136–3142. [PubMed: 8331390]

Swinney DC, & Anthony J (2011). How were new medicines discovered? Nat Rev Drug Discov, 10(7), 507–519. doi:10.1038/nrd3480 [PubMed: 21701501]

Takenaka T, Hiruma H, Hori H, Hashimoto Y, Ichikawa T, & Kawakami T (2003). Fatty acids as an energy source for the operation of axoplasmic transport. Brain Research, 972(1–2), 38–43. doi:10.1016/s0006-8993(03)02481-8 [PubMed: 12711076]

Terry AV Jr., Gearhart DA, Beck WD Jr., Truan JN, Middlemore ML, Williamson LN, . . . Buccafusco JJ (2007). Chronic, intermittent exposure to chlorpyrifos in rats: protracted effects on axonal transport, neurotrophin receptors, cholinergic markers, and information processing. J Pharmacol Exp Ther, 322(3), 1117–1128. doi:10.1124/jpet.107.125625 [PubMed: 17548533]

Tobe BTD, Crain AM, Winquist AM, Calabrese B, Makihara H, Zhao WN, . . . Snyder EY (2017). Probing the lithium-response pathway in hiPSCs implicates the phosphoregulatory set-point for a cytoskeletal modulator in bipolar pathogenesis. Proc Natl Acad Sci U S A, 114(22), E4462–E4471. doi:10.1073/pnas.1700111114 [PubMed: 28500272]

Tucker D, Lu Y, & Zhang Q (2018). From Mitochondrial Function to Neuroprotection-an Emerging Role for Methylene Blue. Mol Neurobiol, 55(6), 5137–5153. doi:10.1007/s12035-017-0712-2 [PubMed: 28840449]

Valvassori SS, Dal-Pont GC, Resende WR, Varela RB, Peterle BR, Gava FF, . . . Quevedo J (2017). Lithium and Tamoxifen Modulate Behavior and Protein Kinase C Activity in the Animal Model of Mania Induced by Ouabain. Int J Neuropsychopharmacol, 20(11), 877–885. doi:10.1093/ijnp/pyx049 [PubMed: 29020306]

Vincent F, Loria P, Pregel M, Stanton R, Kitching L, Nocka K, . . . Peakman MC (2015). Developing predictive assays: the phenotypic screening “rule of 3”. Sci Transl Med, 7(293), 293ps215. doi:10.1126/scitranslmed.aab1201

Wen Y, Li W, Poteet EC, Xie L, Tan C, Yan LJ, . . . Yang SH (2011). Alternative mitochondrial electron transfer as a novel strategy for neuroprotection. J Biol Chem, 286(18), 16504–16515. doi:10.1074/jbc.M110.208447 [PubMed: 21454572]

Widmaier E, Raff H, & Strang K (2007). Vander’s Human Physiology (11 ed). New York: McGraw-Hill.

Won E, & Kim YK (2017). An Oldie but Goodie: Lithium in the Treatment of Bipolar Disorder through Neuroprotective and Neurotrophic Mechanisms. Int J Mol Sci, 18(12). doi:10.3390/ijms18122679

Worek F, Wille T, Koller M, & Thiermann H (2016). Toxicology of organophosphorus compounds in view of an increasing terrorist threat. Arch Toxicol, 90(9), 2131–2145. doi:10.1007/s00204-016-1772-1 [PubMed: 27349770]

Yang X, Naughton SX, Han Z, He M, Zheng YG, Terry AV Jr., & Bartlett MG (2018). Mass Spectrometric Quantitation of Tubulin Acetylation from Pepsin-Digested Rat Brain Tissue Using a Novel Stable-Isotope Standard and Capture by Anti-Peptide Antibody (SISCAPA) Method. Anal Chem, 90(3), 2155–2163. doi:10.1021/acs.analchem.7b04484 [PubMed: 29320166]

Zabrecky JR, & Cole RD (1982). Effect of ATP on the kinetics of microtubule assembly. J Biol Chem, 257(8), 4633–4638. [PubMed: 7068656]

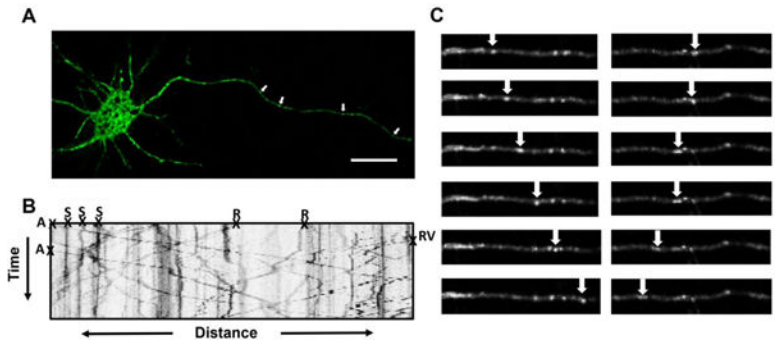

Figure 1.

Methods for testing compounds for their ability to affect axonal transport in vitro. **(A)** Representative image demonstrating successful transfection with pEGFP-n1-APP in rat primary cortical neurons. Arrows indicate membrane-bound organelles (MBOs), scale bar=20μm. **(B)** Kymograph generated from images captured at a rate of one frame every 2s for 3 min demonstrating movement of pEGFP-n1-APP labeled MBOs. MBOs are categorized in 1 of 4 ways: anterograde (A), retrograde (R), stationary (S), or Reversal (RV). **(C)** Representative frames demonstrating progression of MBOs moving in the anterograde and retrograde directions.

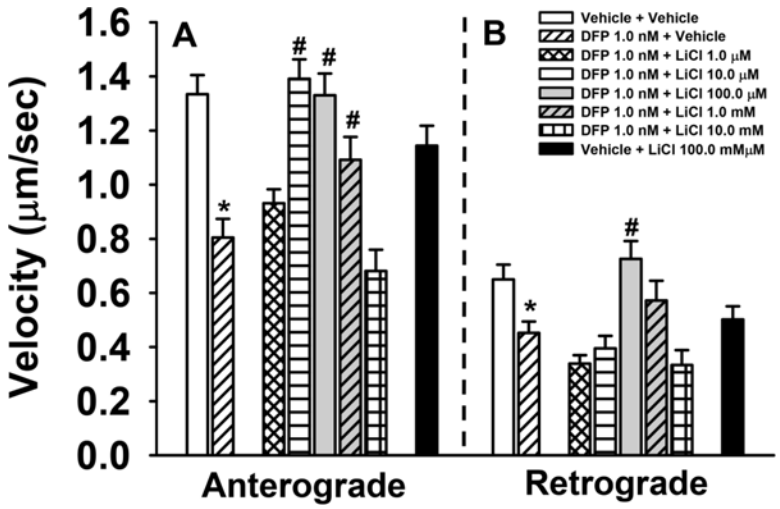

Figure 2.

Effects of Lithium Chloride (LiCl) on DFP-related impairments in axonal transport in rat primary cortical neurons. **(A)** LiCl attenuates DFP-induced anterograde axonal transport deficits across a range of concentrations (10μM-1mM). (**B)** 100μM LiCl attenuates DFP-induced deficits in retrograde axonal transport. Histograms depict the mean ±SEM of all MBOs measured per treatment: anterograde transport, n= 55–284 MBOS and a total of 1289 MBOs analyzed; retrograde n=20–140 MBOs and a total of 751 MBOs analyzed. The MBOs analyzed were obtained from 14–21 individual neurons from 3–5 independent experiments. #= $p<0.05$ compared to DFP *=$p<0.05$ compared to Vehicle.

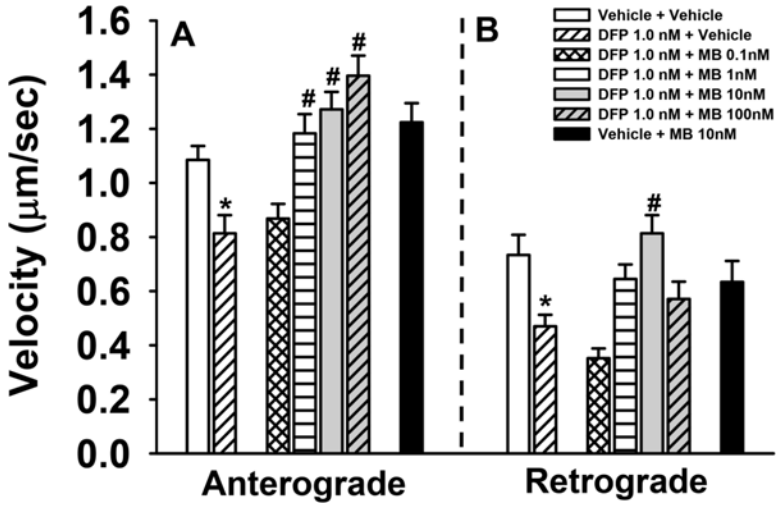

Figure 3.

Effects of methylene chloride (MB) on DFP-related impairments in axonal transport in rat primary cortical neurons. **(A)** MB attenuates DFP-induced anterograde axonal transport deficits across a range of concentrations (1nM-100nM). **(B)** 10nM MB attenuates DFP-induced deficits in retrograde axonal transport. Histograms depict the mean ±SEM of all MBOs measured per treatment: anterograde transport, n= 126–225 MBOs and a total of 1278 MBOs analyzed; retrograde n=78–137 MBOs and a total of 665 MBOs analyzed. The MBOs analyzed were obtained from 14–17 individual neurons from 3–5 independent experiments. #= $p<0.05$ compared to DFP *=$p<0.05$ compared to Vehicle.

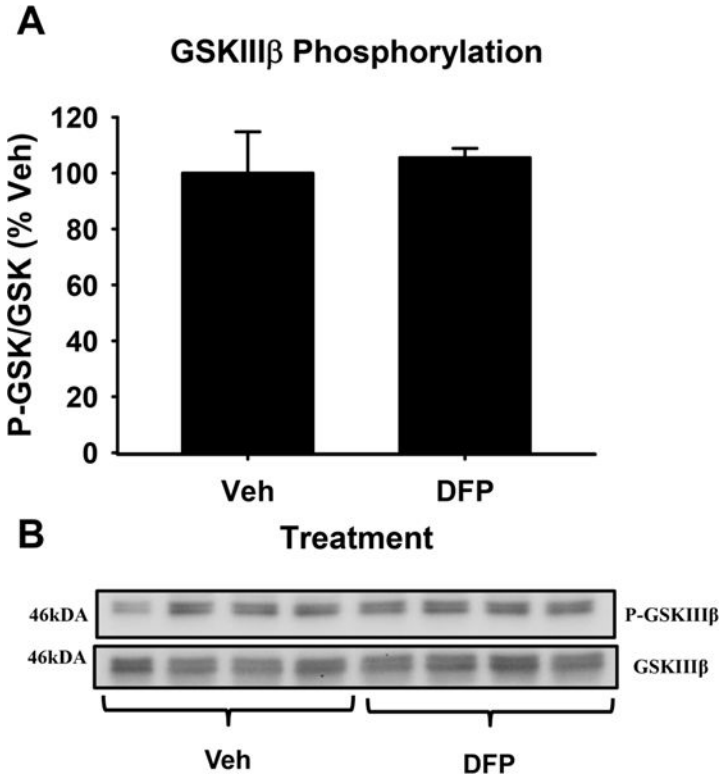

Figure 4.

GSKIIIβ phosphorylation after DFP exposure. Histograms depicting levels of GSKIIIβ phosphorylation (ser9) after 24hr incubation with vehicle or 1.0 nM DFP (A). Immunoblots for P- GSKIIIβ (ser9) and total GSKIIIβ from primary cortical neurons (B). Each bar represents mean ± S.E.M., n=4 with significance assessed at $p<0.05$.

Table 1.

Additional Axonal Transport-Related Measurements (A)

		Directional Movements						
Compound	**Concentration**	**Anterograde**	**Retrograde**	**Stationary**	**Reversals**	**APP Particles**	**Pause Frequency**	**Pause Duration**
	µM	**% of All Particles**	**% of All Particles**	**% of All Particles**	**% of All Particles**	**# of MBOs/mm**	**# pauses/3min**	**sec**
Vehicle	0.0	29.0± 4.57	18.4± 1.84	46.5± 4.00	6.1± 1.44	0.179± 0.0145	0.565± 0.0687	36.317± 2.609
DFP 1.0 nM Plus:								
Lithium Chloride	0.0	22.5± 3.03	16.2± 2.02	57.5± 3.35	3.8± 0.975	0.186± 0.0128	*0.946±0.0714	42.862± 2.454
	1.0	32.6± 3.69	13.0± 2.00	48.3± 3.59	6.1±1.39	#0.224± 0.0138	1.199± 0.0696	41.882± 1.693
	10.0	32.2± 3.65	15.3± 2.19	47.1± 3.54	5.5±0.921	0.181± 0.0138	1.071± 0.0738	36.551± 1.736
	100.0	32.5± 2.87	17.8± 2.97	44.4± 2.94	5.3± 1.66	0.166± 0.0168	0.687± 0.0981	32.244± 2.577
	1000.0	33.3± 5.53	19.3± 4.15	39.8± 4.65	7.6± 2.47	0.179± 0.0224	0.931 ±0.0893	39.746± 2.848
	10000.0	24.4± 7.06	8.3± 3.02	59.4± 6.59	7.9± 2.19	#0.112± 0.0158	0.975± 0.143	39.506± 4.593
Vehicle Plus Lithium Chloride	100.0	34.5± 5.35	20.9± 3.91	#35.8± 4.53	8.8± 1.58	0.175± 0.0171	*1.182±0.0787	34.982 ± 1.465
Vehicle	0.0	37.4 ± 2.93	14.3 ± 2.91	44.2 ± 2.82	4.1 ±0.825	0.219 ± 0.0187	0.679± 0.0685	40.010 ± 2.508
DFP 1.0 nM Plus:								
Methylene Blue	0.0	26.3 ± 4.35	18.8 ± 3.45	49.5 ± 4.69	5.4 ±1.96	0.184 ± 0.0229	0.915± 0.0904	41.081 ± 2.926
	0.0001	21.9 ± 4.17	19.1 ± 2.38	48.9 ± 4.05	10.1 ±2.221	0.179 ± 0.0106	#1.201± 0.0815	35.752 ± 1.695
	0.001	33.5 ± 5.00	18.9 ± 3.12	37.4 ± 4.23	10.3 ±1.99	0.203 ± 0.0181	0.884± 0.0787	34.541 ± 2.050

			Directional Movements									
Compound	**Concentration**		**Anterograde**	**Retrograde**	**Stationary**		**Reversals**		**APP Particles**		**Pause Frequency**	**Pause Duration**
	μM		**% of All Particles**	**% of All Particles**	**% of All Particles**		**% of All Particles**		**# of MBOs/mm**		**# pauses/3min**	**sec**
	0.01		42.0 ± 3.91	18.4 ± 2.52	#33.2 ± 3.41		6.3 ±1.48		0.195 ± 0.0146		0.669± 0.0651	38.127 ± 2.336
	0.1		35.7 ± 5.02	17.0 ± 3.62	44.3 ± 3.80		3.0 ±0.874		0.192 ± 0.0165		0.759± 0.0810	40.406 ± 2.538
Vehicle Plus Methylene Blue	0.01		#44.7 ± 3.97	16.5 ± 309	#30.8 ± 3.94		8.1 ±1.95		0.167 ± 0.0138		0.941± 0.0818	38.711 ± 2.368

Each value represents the mean ± s.e.m obtained from 14–21 individual neurons from 3–5 separate experiments with 1–6 neurons per individual experiment.

* = significantly ($p<0.05$) different from vehicle control

= significantly ($p<0.05$) different from 1nM DFP.